J Wood Sci (2004) 50:197–208
DOI 10.1007/s10086-003-0556-4

ORIGINAL ARTICLE

Hiroyuki Yamamoto

Role of the gelatinous layer on the origin of the physical properties of the tension wood

Received: August 28, 2002 / Accepted: May 6, 2003

Abstract To discuss the role of the gelatinous layer (G-layer) on the origins of the physical properties peculiar to the tension wood fiber (TW fiber), the deformation process of an isolated TW fiber caused by a certain biomechanical state change was formulated mathematically. The mechanical model used in the present formulation is a four-layered hollow cylinder having the compound middle lamella (CML), the outer layer of the secondary wall (S1) and its middle layer (S2), and the G-layer (G) as an innermost layer. In the formulation, the reinforced matrix mechanism was applied to represent the mechanical interaction between the cellulose microfibril (CMF) as a framework bundle and the amorphous substance as a matrix skeleton in each layer. The model formulated in the present study is thought to be useful to investigate the origins of extensive longitudinal drying shrinkage, large tensile growth stress, and a high axial elastic modulus, which are rheological properties peculiar to the TW. In this article, the detailed process of the mathematical formulation is described. In a subsequent article, some TW properties from a 70-year-old Kohauchiwakaede (*Acer sieboldianum* Miq.) will be analyzed using the newly developed model.

Key words Gelatinous fiber · Tension wood · Cell wall · Reaction wood · Growth stress

Introduction

Tension wood (TW) consists of abnormal tissue called gelatinous fiber (G-fiber) because it contains a gelatinous layer (G-layer) as the innermost layer of the secondary wall. The TW often shows characteristic behavior that is different from the normal wood (NW). A high-tensile growth stress is generated on the surface of the xylem in the TW region that often becomes ten times as large as that in the NW region.[1,2] The longitudinal Young's modulus of the TW becomes significantly higher than that of the NW.[1,3] Furthermore, the axial shrinkage in the TW tends to exceed more than 1% during water desorption,[3] while that in the NW becomes less than 0.5%. Some authors attribute these behaviors to the intrinsic properties of the G-fiber.[1,3]

On the other hand, more than a few researchers believe that the G-layer is mechanically too compliant to bear a large stress generation. They base their argument on the facts that the G-layer is often convoluted in the lumen of the transverse section that is sampled from the water-swollen block, and it can be easily peeled off the lignified layer in the same direction during microtoming. This gives the impression that it is attached only loosely to the remainder of the secondary wall.[4] From those observations, they consider that the various characteristics of the TW should be attributed not to the flexible G-layer but to the relatively thicker outer layer of the secondary wall (S1),[5] and/or to the relatively thinner middle layer of the secondary wall (S2) whose microfibril angle (MFA) is expected to be more or less different from that in the NW fiber.[6,7]

It is impossible to adjudge which possibility holds until we succeed in directly measuring the mechanical properties of the G-layer and the lignified layer which requires isolating them from each other. However, it may be quite natural to consider that the lignified layer in the G-fiber would be essentially same as that in the NW fiber, because there is no specific difference in anatomical and chemical aspects between them as pointed by Okuyama et al.[1] Thus, the author expects that characteristic behaviors peculiar to the TW may be attributed to the G-layer.

Simulation using a wood fiber model is one of the most effective methods to estimate the internal properties and fine structures of each constituent material in wood cell walls.[8,9] In our previous studies, we developed a wood fiber model consisting of the compound middle lamella (CML), S1 and S2. A basic formula was derived to simulate the deformation process of an isolated wood fiber when a

H. Yamamoto (✉)
School of Bioagricultural Sciences, Nagoya University, Chikusa, Nagoya 464-8601, Japan
Tel. +81-52-789-4152; Fax +81-52-789-4150
e-mail: hiro@agr.nagoya-u.ac.jp

certain biomechanical change occurs, such as lignin deposition,[10,11] water adsorption,[12,13] or external load induction.[9,14] The basic formula contained several parameters that were derived from the composite structure of the cell wall layer. When comparing the simulated results with the experimental one, concrete values need to be assigned to the parameters in a rational manner. We consider that those values reflect intrinsic information on the internal properties and fine structure of cell wall constituents.

The objective of the present study was to clarify the role of the G-layer in the origin of characteristic behaviors of the TW, and then, to improve our previous wood fiber model[12,15] into a four-layered model having the G-layer as the innermost layer. In the present article, the detailed process of the formulation on the deformation process of the G-fiber model which is induced by a certain biomechanical state changes is described. In a subsequent article, some TW properties of 70-year-old kohauchiwakaede (*Acer sieboldianum* Miq.) will be analyzed by using the newly developed model, including a high-tensile growth stress generation, a large longitudinal Young's modulus, and a large axial shrinkage due to water desorption.

Formulation of the deforming wood

Wood fiber model

Figure 1 shows a schematic model of the typical G-fiber which consists of the CML, the S1, the S2, and the G-layers. Each layer can be approximated as a "two-phase structure", specifically the unidirectional reinforcing element of the polysaccharide framework and the encrusting matrix (MT) of lignin–hemicellulose compound. The former is mainly composed of highly crystallized cellulose microfibril (CMF), which is oriented in a certain direction to the fiber axis in each layer except the CML. This makes the secondary wall and the G-layer mechanically anisotropic. On the other hand, in cases in which the orientation of the CMF is randomly distributed in the CML, it is considered to be mechanically isotropic.

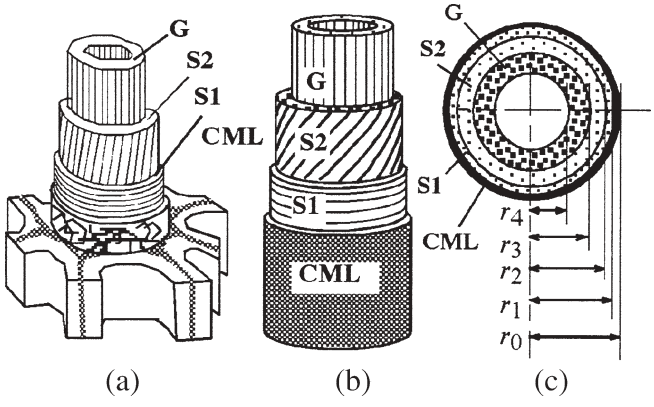

Fig. 1. Multilayered structure of the gelatinous fiber (**a**), its mechanical model (**b**), and the crosscut surface (**c**). Each fiber consists of the compound middle lamella (*CML*), the outermost layer of the secondary wall (*S1*), its middle layer (*S2*), and the gelatinous layer (*G*)

In the case of softwood secondary wall, oriented polyose, such as (acetyl-) glucomannan, is often arranged along and around the CMF, forming the polysaccharide framework with the highly crystallized CMF. No oriented polyose has been detected in the hardwood cell wall.[16–18] Disoriented polyose, that is mainly xylan, is blended with lignin, forming the isotropic skeleton of the MT substance.

In the present study, a single G-fiber is simplified into a complex hollow cylinder consisting of the CML, the S1, the S2, and the G-layers, as shown in Fig. 1b.

Constitutive equations

Under low magnification, the reinforcing element of the polysaccharide framework is spatially dispersed uniformly in each cell wall layer to form the framework bundle. Similarly, the lignin–hemicellulose compound is diffused in each layer forming the isotropic MT skeleton. Therefore, it is considered that both the framework bundle and the MT skeleton occupy the same domain in the macroscopic limit. Based on such an idea, Barber and Meylan hypothesized the mechanical interaction between the polysaccharide framework and the lignin–hemicellulose MT in each layer as the following conditions: [12,19,20]

$$\sigma_{ij} = \sigma_{ij}^{f} + \sigma_{ij}^{m}, \qquad \varepsilon_{ij} = \varepsilon_{ij}^{f} = \varepsilon_{ij}^{m} \tag{1}$$

where σ_{ij}^{f}, σ_{ij}^{m}, and σ_{ij} are the stress tensors in the framework bundle, MT skeleton, and cell wall layer as a whole, respectively. ε_{ij}^{f}, ε_{ij}^{m}, and ε_{ij}, on the other hand, are their respective strains.

In the present study, the deformation of the wood fiber model is assumed to be symmetric with respect to the central axis (see the condition C4). Thus, we can express the fact that torsional deformation of an individual fiber is completely restricted by the force of binding fibers inside the wood specimen. Then a cylindrical coordinate system (O-ℓtr, where ℓ, t, and r represent longitudinal, tangential, and radial components, respectively) can be applied to the present model as shown in Fig. 2a.

A visible deformation induced at each point in the cell wall is expressed by the observable strain tensor components (ε_{ij}, where $i, j = \ell$, t, r) in the O-ℓtr coordinate system. The stress component induced in the MT skeleton of each layer (σ_{ij}^{m}) is related to the observable strain component caused in the matrix skeleton (ε_{ij}^{m}, where $i, j = \ell$, t, r) as the following constitutive equation:

$$\sigma_{ij}^{m} = C_{ijkl}^{m}\left(\varepsilon_{kl}^{m} - \alpha_{kl}^{m}\right) \tag{2}$$

C_{ijkl}^{m} is an elastic constant tensor, and α_{kl}^{m} is a tensor of internal expansion which is caused by a certain biomechanical change. α_{kl}^{m} is observed such that in each layer, $\alpha_{kl}^{m} = \varepsilon^{m}\delta_{kl}$, where δ_{kl} is Kronecker's symbol. ε^{m} is a scalar. C_{ijkl}^{m} and α_{kl}^{m} are both assumed to be isotropic. The elastic constants of the isotropic MT skeleton (nonzero terms) are denoted as follows:

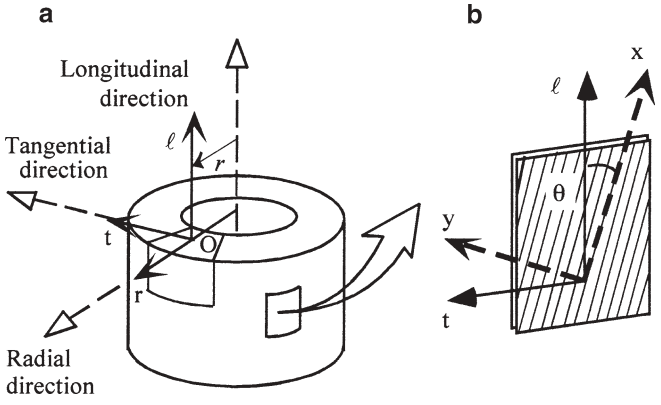

Fig. 2a,b. Coordinate system used in the formulation. **a** O-ℓtr local orthogonal coordinate system. **b** Flat board element of the CMF framework bundle. O (in **a**) is an arbitrary point in the cell wall. Direction of *x*-axis (in **b**) is parallel to the CMF molecular chains in the S1 or S2 layers

$$C^{\mathrm{m}}_{\ell\ell\ell\ell} = C^{\mathrm{m}}_{\mathrm{tttt}} = C^{\mathrm{m}}_{\mathrm{rrrr}} = \frac{1}{3}(K + 2S),$$
$$C^{\mathrm{m}}_{\ell\ell\mathrm{tt}} = C^{\mathrm{m}}_{\mathrm{ttrr}} = C^{\mathrm{m}}_{\mathrm{tt}\ell\ell} = C^{\mathrm{m}}_{\ell\ell\mathrm{rr}} = C^{\mathrm{m}}_{\mathrm{rr}\ell\ell} = C^{\mathrm{m}}_{\mathrm{rrtt}} = \frac{1}{3}(K - S),$$
$$C^{\mathrm{m}}_{\mathrm{trtr}} = C^{\mathrm{m}}_{\mathrm{r}\ell\mathrm{r}\ell} = C^{\mathrm{m}}_{\ell\mathrm{t}\ell\mathrm{t}} = \frac{1}{2}S \tag{3}$$

where $K = 3\lambda + 2\mu$, $S = 2\mu$. λ and μ are Lame's constants.

Figure 2b shows a small flat-board element of the framework bundle in the S2 layer, provided that the positive direction of normal axis (z-axis) is coincident with the radial direction (r-axis) of the fiber model. In this model, the CMF and other oriented polyose in the S2 layer are assumed to be oriented in an S-helix at an angle of θ, and the one in the S1 layer is assumed to be aligned normally to the fiber axis. The relationship between stress ($\sigma^{\mathrm{f}*}_{ij}$) and strain ($\varepsilon^{\mathrm{f}*}_{ij}$) components induced in the framework bundle of each layer of the secondary wall can be written as the following constitutive equation in the O-*xyz* orthogonal coordinate system:

$$\sigma^{\mathrm{f}*}_{ab} = C^{\mathrm{f}*}_{abcd}\left(\varepsilon^{\mathrm{f}*}_{cd} - \alpha^{\mathrm{f}*}_{cd}\right) \tag{4}$$

where $C^{\mathrm{f}*}_{abcd}$ is the elastic constant of the framework bundle in each layer in the O-*xyz* coordinate system. $\alpha^{\mathrm{f}*}_{ab}$ is an internal expansive strain, caused by a certain biomechanical change, that is a diagonal tensor whose components are

$$\mathrm{diag}\left(\alpha^{\mathrm{f}*}_{ab}\right) = \left(\varepsilon^{\mathrm{f}}, \varepsilon^{\mathrm{f}'}, \varepsilon^{\mathrm{f}'}\right)$$

where ε^{f} and $\varepsilon^{\mathrm{f}'}$ are the internal expansive strains induced in the framework bundle in the directions parallel and perpendicular to the cellulose molecular chain, respectively.

We supposed that the framework bundle is considerably compliant in its transverse direction. Therefore, all shear moduli, Poisson's ratios, and the Young's modulus in the transverse direction are small enough to be neglected. This means that the CMF including other oriented polysaccharide cannot be kept in a bundle shape without a reinforcing agent. The reinforcing agent is considered to be the lignin–hemicellulose isotropic matrix. Then, we may consider the stiffness components $C^{\mathrm{f}*}_{abcd}$ are all nil except $C^{\mathrm{f}*}_{\mathrm{xxxx}}$ ($=E$).

By transforming the coordinate system from O-*xyz* into O-ℓtr system, Eq. 4 is rewritten into a new expression as follows:

$$\sigma^{\mathrm{f}}_{ij} = C^{\mathrm{f}}_{ijkl}\left(\varepsilon^{\mathrm{f}}_{kl} - \alpha^{\mathrm{f}}_{kl}\right) \tag{5}$$

where

$$C^{\mathrm{f}}_{ijkl} = R_{ia}R_{jb}R_{kc}R_{ld}C^{\mathrm{f}*}_{abcd}, \qquad \alpha^{\mathrm{f}}_{ij} = R_{ia}R_{jb}\alpha^{\mathrm{f}*}_{ab} \tag{6}$$

R_{ij} is a transformation matrix between both coordinate systems. The nonzero terms of the stiffness components of the framework bundle (C^{f}_{ijkl}) are expressed as

$$C^{\mathrm{f}}_{\ell\ell\ell\ell} = c^4E, \quad C^{\mathrm{f}}_{\ell\ell\mathrm{tt}} = C^{\mathrm{f}}_{\mathrm{tt}\ell\ell} = c^2s^2E, \quad C^{\mathrm{f}}_{\ell\ell\ell\mathrm{t}} = C^{\mathrm{f}}_{\ell\mathrm{t}\ell\ell} = -c^3sE,$$
$$C^{\mathrm{f}}_{\mathrm{tttt}} = s^4E, \quad C^{\mathrm{f}}_{\mathrm{tt}\ell\mathrm{t}} = C^{\mathrm{f}}_{\ell\mathrm{ttt}} = -cs^3E, \quad C^{\mathrm{f}}_{\ell\mathrm{t}\ell\mathrm{t}} = c^2s^2E,$$
$$\alpha^{\mathrm{f}}_{\ell\ell} = \varepsilon^{\mathrm{f}}c^2 + \varepsilon^{\mathrm{f}'}s^2, \quad \alpha^{\mathrm{f}}_{\mathrm{tt}} = \varepsilon^{\mathrm{f}}s^2 + \varepsilon^{\mathrm{f}'}c^2, \quad \alpha^{\mathrm{f}}_{\ell\mathrm{t}} = -\left(\varepsilon^{\mathrm{f}} - \varepsilon^{\mathrm{f}'}\right)cs \tag{7}$$

provided that we considered $C^{\mathrm{f}}_{ijkl} = C^{\mathrm{f}}_{jikl} = C^{\mathrm{f}}_{ijlk}$ and $C^{\mathrm{f}}_{ijkl} = C^{\mathrm{f}}_{klij}$, where $c = \cos\varphi$, $s = \sin\varphi$, and E is Young's modulus of the framework bundle in the direction along the cellulose molecular chain. E, S, ε^{m}, ε^{f}, ρ ($=r_{\mathrm{out}}/r_{\mathrm{in}}$), and φ take respective values in each layer as assumed in Table 1. They are not unknown values to be solved but known constants to be given in advance.[8,13] S is the shear modulus ($\times 2$) of the matrix skeleton in each layer. In the same way as E, S takes a respective value in each layer. S is denoted as S_0, S_1, S_2, and S_3 in the CML, S1, S2, amd G-layers, respectively.

By rearranging Eqs. 1 using Eqs. 2, 3, 5, and 7, and considering the compatibility of strains for the axisymmetrical deformation without torsion,

$$\varepsilon_{\mathrm{r}} - \varepsilon_{\mathrm{t}} = r\frac{d\varepsilon_{\mathrm{t}}}{dr}$$

we obtain

$$\sigma_{\ell} = -K\varepsilon^{\mathrm{m}} - Ec^2\varepsilon^{\mathrm{f}} + \left\{\frac{1}{3}(K + 2S) + Ec^4\right\}\varepsilon_{\ell} + \left\{\frac{2}{3}(K - S) + Ec^2s^2\right\}\varepsilon_{\mathrm{t}} + \frac{1}{3}(K - S)r\frac{d\varepsilon_{\mathrm{t}}}{dr},$$
$$\sigma_{\mathrm{t}} = -K\varepsilon^{\mathrm{m}} - Es^2\varepsilon^{\mathrm{f}} + \left\{\frac{1}{3}(K - S) + Ec^2s^2\right\}\varepsilon_{\ell} + \left\{\frac{1}{3}(2K + S) + Es^4\right\}\varepsilon_{\mathrm{t}} + \frac{1}{3}(K - S)r\frac{d\varepsilon_{\mathrm{t}}}{dr},$$
$$\sigma_{\mathrm{r}} = -K\varepsilon^{\mathrm{m}} + \frac{1}{3}(K - S)\varepsilon_{\ell} + \frac{1}{3}(2K + S)\varepsilon_{\mathrm{t}} + \frac{1}{3}(K + 2S)r\frac{d\varepsilon_{\mathrm{t}}}{dr},$$
$$\sigma_{\ell\mathrm{t}} = -Ecs\left(\varepsilon_{\ell}c^2 + \varepsilon_{\mathrm{t}}s^2 - \varepsilon^{\mathrm{f}}\right), \qquad \sigma_{\mathrm{tr}} = \sigma_{\mathrm{r}\ell} = 0 \tag{8}$$

where $\sigma_{\ell} \equiv \sigma_{\ell\ell}$, $\sigma_{\mathrm{t}} \equiv \sigma_{\mathrm{tt}}$, $\sigma_{\mathrm{r}} \equiv \sigma_{\mathrm{rr}}$, $\varepsilon_{\ell} \equiv \varepsilon_{\ell\ell}$, $\varepsilon_{\mathrm{t}} \equiv \varepsilon_{\mathrm{tt}}$, $\varepsilon_{\mathrm{r}} \equiv \varepsilon_{\mathrm{rr}}$. r is a radial distance from the central axis. Among the shear

Table 1. List of the parameters in the basic formulae A and B

Layer	φ	r_{in}	r_{out}	ρ	S	E	P_{in}	P_{out}	L	ε^m	ε^f
CML	–	r_1	r_0 $(=r_1 + h)$	$\rho_0\left(=\frac{r_0}{r_1}\right)$	S_0	E_0 $(=0)$	P_1	P_0 $(=0)$	L_0	0	0
S1	90 deg	r_2	r_1	$\rho_1\left(=\frac{r_1}{r_2}\right)$	S_1	E_1	P_2	P_1	L_1	ε_1^m	ε_1^f
S2	θ	r_3	r_2	$\rho_2\left(=\frac{r_2}{r_3}\right)$	S_2	E_2	P_3	P_2	L_2	ε_2^m	ε_2^f
G	0 deg	r_4	r_3	$\rho_3\left(=\frac{r_3}{r_4}\right)$	S_3	E_3	P_4 $(=0)$	P_3	L_3	ε_3^m	ε_3^f

φ, the microfibril angle; r_{in}, inner radius of each layer; r_{out}, outer radius of each layer; $\rho = r_{out}/r_{in}$; S, shear modulus ($\times 2$) of the matrix skeleton; E, Young's modulus of the framework bundle in the direction along the cellulose molecular chain; P_{in}, inner pressure; P_{out}, outer pressure; L, see Eqs. 10; ε^m, inelastic strains in the matrix skeleton; ε^f, inelastic strains of the framework bundle in the direction parallel to cellulose molecular chains; CML, compound middle lamella; $G = E/S$; $G_1 = E_1/S_1$; $G_2 = E_2/S_2$; $G_3 = E_3/S_3$; $Q = F/E_1$; $F = S_0 \cdot h/r_1$; $M = S_2/S_1$; $N = S_3/S_2$

stress components, only $\sigma_{\ell t}$ is not null, which is an inevitable consequence from the assumption of the axisymmetrical deformation, i.e., $\varepsilon_{\ell t} = 0$. In this study, stress equilibrium for axisymmetrical deformation was assumed as follows:

$$\sigma_t - \sigma_r = r\frac{d\sigma_r}{dr} \tag{9}$$

Deriving the basic equations

Assumptions

The dimensional change of the wood fiber model can be expressed as a set of normal strains, namely, ε_ℓ in the longitudinal direction, and $\varepsilon_t(r)|_{r=r_0}$, $\varepsilon_t(r)|_{r=r_1}$, $\varepsilon_t(r)|_{r=r_2}$, $\varepsilon_t(r)|_{r=r_3}$, and $\varepsilon_t(r)|_{r=r_4}$ in the tangential directions at the respective radius. In the same way as described in previous work,[11,12,14] based on Eqs. 8, we solve ε_ℓ, $\varepsilon_t(r)|_{r=r_0}$, $\varepsilon_t(r)|_{r=r_1}$, $\varepsilon_t(r)|_{r=r_2}$, $\varepsilon_t(r)|_{r=r_3}$, and $\varepsilon_t(r)|_{r=r_4}$ under the conditions C1, C2, C3, and C4, and assumptions A1, A2, and A3:

C1. ε_ℓ is constant for all r. This is based on the assumption that the wood fiber model is an infinitely long cylinder in the ℓ-direction. We denote ε_ℓ as ε_L hereafter.

C2. $[\sigma_r(r)]_{r=r_4} = -P_4$, $[\sigma_r(r)]_{r=r_0} = -P_0$. $P_0 = P_4 = 0$. These boundary conditions mean there are no internal and external pressures acting on the wood fiber model (see Table 1).

C3. The external force (P_L) induced parallel to the wood fiber model satisfies the following equation:

$$P_L = 2\pi L = \int_{\substack{\text{crosscut}\\\text{surface}}} \sigma_l dA = \int_{\substack{\text{crosscut}\\\text{surface}}} \sigma_l r dr d\theta = 2\pi \int_{r_4}^{r_0} r\sigma_l(r) dr \tag{10}$$

C4. The deformation of the wood fiber model is assumed to be symmetric with respect to the central axis.

In addition to the conditions, the assumptions A1, A2, and A3 were made at processing:

A1. $K \gg S$, so that S/K is enough small to be negligible in each layer. This hypothesizes that the bulk modulus of the MT skeleton (K) is larger than S. This postulates that the Poisson's ratio of the matrix skeleton is almost 0.5, similar to a kind of elastomer.

A2. It is considered that E, S, ε^m, ε^f, and ρ $(=r_{out}/r_{in})$ tend to change their values during a certain biophysical change; however, those changes can be neglected in the case that biomechanical changes were infinitesimally small.

A3. $E = 0$ in Eq. 7 in the CML. Namely, $E_0 = 0$. This does not mean that there is no oriented polysaccharide framework in the CML, but means that mechanical contribution of the randomly distributed polysaccharide framework in the CML should be isotropic. For convenience, we assume that S_0 means the shear modulus ($\times 2$) of the CML itself. Moreover, $(h/r_1)^2 \sim 0$, $\varepsilon_0^f = 0$ and $\varepsilon_0^m = 0$ in the CML. These conditions assume that h (thickness of the CML) is smaller than the S1 and the S2 layers.

Basic formula A

Solving the second and third formula in Eqs. 8 for ε_t and $rd\varepsilon_t/dr$, and eliminating the term of σ_t using the equilibrium condition of Eq. 9, we obtain

$$\begin{aligned}
&\left[2S + Es^4 + u\left(S + 2Es^4\right)\right]\varepsilon_t = 3S \cdot \varepsilon^m + (1 + 2u)E \cdot s^2 \cdot \varepsilon^f \\
&\quad - \left[S + Ec^2s^2 + u\left(-S + 2Ec^2s^2\right)\right]\varepsilon_L + (1 + 2u)r\frac{d\sigma_r}{dr} \\
&\quad + 3u\sigma_r, \\
&\left[2S + Es^4 + u\left(S + 2Es^4\right)\right]r\frac{d\varepsilon_t}{dr} = 3E \cdot s^4 \cdot \varepsilon^m \\
&\quad -(2 + u)E \cdot s^2 \cdot \varepsilon^f + \left(2 - 3s^2 + u\right)E \cdot s^2 \cdot \varepsilon_L \\
&\quad - (2 + u)r\frac{d\sigma_r}{dr} + 3Gus^4\sigma_r
\end{aligned} \tag{11}$$

where $u = S/K$ and $G = E/S$. Moreover, combining them by eliminating the term of ε_t, we obtain a differential equation of r:

Table 2. List of the coefficients in the basic formulae A and B

Layer	Location	Γ	Λ	X	Δ	Ω	Φ	Σ
CML	$r = r_0$	$\Gamma'_0\ (=1)$	$\Lambda'_0\ (=2)$	$X'_0\ (=3)$	$\Delta'_0\ (=0)$	$\Omega_0\ (=1)$	$\Phi_0\ (=1)$	$\Sigma_0(=0)$
	$r = r_1$	$\Gamma_0\ (=1)$	$\Lambda_0\ (=2)$	$X_0\ (=3)$	$\Delta_0\ (=0)$			
S1	$r = r_1$	Γ'_1	Λ'_1	X'_1	Δ'_1	Ω_1	Φ_1	Σ_1
	$r = r_2$	Γ_1	Λ_1	X_1	Δ_1			
S2	$r = r_2$	Γ'_2	Λ'_2	X'_2	Δ'_2	Ω_2	Φ_2	Σ_2
	$r = r_3$	Γ_2	Λ_2	X_2	Δ_2			
G	$r = r_3$	$\Gamma'_3\ (=1)$	$\Lambda'_3\ (=2)$	$X'_3\ (=3)$	$\Delta'_3\ (=0)$	Ω_3	$\Phi_3\ (=1)$	Σ_3
	$r = r_4$	$\Gamma_3\ (=1)$	$\Lambda_3\ (=2)$	$X_3\ (=3)$	$\Delta_3\ (=0)$			

$$\begin{aligned}(1+2u)r^2\frac{d^2\sigma_r}{dr^2} + 3(1+2u)r\frac{d\sigma_r}{dr} - 3Gus^4\sigma_r \\ = 3E\cdot s^4\varepsilon^m - (2+u)E\cdot s^2\varepsilon^f + E\cdot s^2(2-3s^2+u)\varepsilon_L\end{aligned} \tag{12}$$

General solution of Eq. 12 is given as

$$\begin{aligned}\sigma_r = {} & C_1 r^{\alpha-1} + C_2 r^{-\alpha-1} - \frac{1}{1+2u}\cdot\frac{1}{2\alpha}\Big[3E\cdot s^4\varepsilon^m \\ & - (2+u)E\cdot s^2\varepsilon^f + E\cdot s^2(2-3s^2+u)\varepsilon_L\Big] \\ & \times\left[\frac{1}{1+\alpha} - \left(\frac{r^{\alpha-1}-1}{\alpha-1}\right)\right]\end{aligned} \tag{13}$$

where C_1 and C_2 are integral constants, and α is described as follows:

$$\alpha = \sqrt{1+3G\cdot s^4\frac{u}{1+2u}} = \sqrt{1+3G\cdot s^4\frac{S}{K+2S}}$$

Based on the assumption A1, we impose the following conditions:

$$u \to +0 \quad \text{then} \quad \alpha \to 1+0$$

which yields

$$\lim_{\alpha\to 1+0}\frac{r^{\alpha-1}-1}{\alpha-1} \to \ln r$$

Then, we can simplify the solution of Eq. 13 as follows:

$$\begin{aligned}\sigma_r = {} & C'_1 + C_2 r^{-2} + \frac{1}{2}\Big[3E\cdot s^4\varepsilon^m - 2E\cdot s^2\varepsilon^f \\ & + (2-3s^2)E\cdot s^2\varepsilon_L\Big]\ln r\end{aligned}$$

Under the boundary conditions $[\sigma_r(r)]_{r=r_{in}} = -P_{in}$ and $[\sigma_r(r)]_{r=r_{out}} = -P_{out}$, we can decide the integral constants C'_1 and C_2, and we obtain the following solution:

$$\begin{aligned}\sigma_r = {} & -P_{in} - \frac{\rho^2 - r_{out}^2/r^2}{\rho^2-1}\left\{P_{out} - P_{in} + \frac{1}{2}\Big[3E\cdot s^4\varepsilon^m\right. \\ & \left. - 2E\cdot s^2\varepsilon^f + E\cdot s^2(2-3s^2)\varepsilon_L\Big]\ln\rho\right\} + \frac{1}{2}\Big[3E\cdot s^4\varepsilon^m \\ & - 2E\cdot s^2\varepsilon^f + E\cdot s^2(2-3s^2)\varepsilon_L\Big]\ln\frac{r}{r_{in}}\end{aligned} \tag{14}$$

Then, we substitute the above solution into the first part of Eq. 11, and we obtain basic formula A:

$$\begin{aligned}\Gamma\cdot\varepsilon_L + \Lambda\cdot\varepsilon_t = {} & X\cdot\varepsilon^m + \Delta\cdot\varepsilon^f - 2\frac{1}{(\rho^2-1)}\left(\frac{r_{out}^2}{r^2}\right)\frac{P_{out}}{S} \\ & + 2\frac{1}{(\rho^2-1)}\left(\frac{r_{out}^2}{r^2}\right)\frac{P_{in}}{S}\end{aligned}$$

where

$$\Gamma = 1 + \frac{1}{2}G\cdot s^4 + G\cdot s^2(2-3s^2)\frac{\ln\rho}{(\rho^2-1)}\left(\frac{r_{out}^2}{r^2}\right),$$

$$\Lambda = 2 + G\cdot s^4, \quad X = 3 + \frac{3}{2}G\cdot s^4 - 3G\cdot s^4\frac{\ln\rho}{(\rho^2-1)}\left(\frac{r_{out}^2}{r^2}\right),$$

$$\text{and} \quad \Delta = 2G\cdot s^2\frac{\ln\rho}{(\rho^2-1)}\left(\frac{r_{out}^2}{r^2}\right)$$

Coefficients Γ, Λ, X, and Δ are dependent on G, φ, r, r_{out}, and ρ, provided that these variables take their respective values in each layer as shown in Table 2.

Basic formula B

We solve Eqs. 8 for ε_L and integrate it over the crosscut area of each layer. When integrating it, we assume that ε^m and ε^f are independent of r in the respective layers, and ε_ℓ takes a constant value (ε_L) over the crosscut surface of the cell wall because of condition C1. As a result, we obtain basic formula B:

$$\begin{aligned}\Omega\cdot\varepsilon_L = {} & \Phi\cdot\varepsilon^m + \Sigma\cdot\varepsilon^f + \frac{2}{3}\frac{L}{S\cdot r_{in}^2}\frac{\Lambda}{(\rho^2-1)} \\ & + \frac{2}{3}\frac{\rho^2}{(\rho^2-1)}\frac{P_{out}}{S}[\Gamma]_{r=r_{out}} - \frac{2}{3}\frac{1}{(\rho^2-1)}\frac{P_{in}}{S}[\Gamma]_{r=r_{in}}\end{aligned}$$

where

$$\begin{aligned}\Omega = {} & 1 + \frac{2}{3}G(1-3s^2+3s^4) \\ & - \frac{1}{3}G^2\cdot s^4(2-3s^2)^2\left[\left(\frac{\rho}{\rho^2-1}\ln\rho\right)^2 - \frac{1}{4}\right],\end{aligned}$$

$$\Phi = 1 - G \cdot s^2\left(c^2 - s^2\right) + G^2 \cdot s^6\left(2 - 3s^2\right)\left[\left(\frac{\rho}{\rho^2 - 1}\ln\rho\right)^2 - \frac{1}{4}\right],$$

$$\Sigma = \frac{1}{3}G\left(2 - 3s^2\right) - \frac{2}{3}G^2 \cdot s^4\left(2 - 3s^2\right)\left[\left(\frac{\rho}{\rho^2 - 1}\ln\rho\right)^2 - \frac{1}{4}\right],$$

$$L = \frac{1}{2\pi}\int_{\text{each layer}} \sigma_\ell r \mathrm{d}r\mathrm{d}\theta$$

Coefficients Ω, Φ, and Σ are dependent on G, φ, and ρ, provided that these coefficients take their respective values in each layer as shown in Table 2.

Formulae to describe the deforming G-fiber

In the G-fiber model as the whole, twelve equations are obtained based on the basic formulae A and B. The equations are as follows:

Basic formula A in CML at $r = r_0$ (a0),
Basic formula A in CML at $r = r_1$ (a0′),
Basic formula B in CML (b0),
Basic formula A in S1 at $r = r_1$ (a1),
Basic formula A in S1 at $r = r_2$ (a1′),
Basic formula B in S1 (b1),
Basic formula A in S2 at $r = r_2$ (a2),
Basic formula A in S2 at $r = r_3$ (a2′),
Basic formula B in S2 (b2),
Basic formula A in G at $r = r_3$ (a3),
Basic formula A in G at $r = r_4$ (a3′),
Basic formula B in G (b3).

These equations constitute simultaneous equations whose unknown variables are

$$\varepsilon_{\mathrm{L}},\ \varepsilon_{\mathrm{t}}\big|_{r=r_0},\ \varepsilon_{\mathrm{t}}\big|_{r=r_1},\ \varepsilon_{\mathrm{t}}\big|_{r=r_2},\ \varepsilon_{\mathrm{t}}\big|_{r=r_3},\ \varepsilon_{\mathrm{t}}\big|_{r=r_4};$$
$$P_0,\ P_1,\ P_2,\ P_3,\ P_4;\ L_0,\ L_1,\ L_2,\ L_3$$

According to the assumption A3, Eqs. a0 and a0′ are degenerated by each other, which yields

$$\varepsilon_{\mathrm{t}}\big|_{r=r_0} \approx \varepsilon_{\mathrm{t}}\big|_{r=r_1}$$

Therefore, the unknown variables become

$$\varepsilon_{\mathrm{L}},\ \varepsilon_{\mathrm{t}}\big|_{r=r_1},\ \varepsilon_{\mathrm{t}}\big|_{r=r_2},\ \varepsilon_{\mathrm{t}}\big|_{r=r_3},\ \varepsilon_{\mathrm{t}}\big|_{r=r_4};$$
$$P_0,\ P_1,\ P_2,\ P_3,\ P_4;\ L_0,\ L_1,\ L_2,\ L_3$$

To solve Eqs. a0′–a3′, and Eqs. b1–b3 for the unknown variables, the following conditions based on conditions C2 and C3 are imposed:

$$P_0 = 0 \quad (\mathrm{c1}), \quad P_4 = 0 \quad (\mathrm{c2}), \quad L = L_0 + L_1 + L_2 + L_3 \quad (\mathrm{c3})$$

The unknown variables explicitly required in our study are ε_{L}, $\varepsilon_{\mathrm{t}}|_{r=r_1}$, $\varepsilon_{\mathrm{t}}|_{r=r_2}$, $\varepsilon_{\mathrm{t}}|_{r=r_3}$, and $\varepsilon_{\mathrm{t}}|_{r=r_4}$. Thus, by eliminating the unknown variables P_0, P_1, P_2, P_3, P_4, L_0, L_1, L_2, L_3, and L in the following manner, we degenerated the simultaneous equations into simpler ones in which the unknown variables are ε_{L}, $\varepsilon_{\mathrm{t}}|_{r=r_1}$, $\varepsilon_{\mathrm{t}}|_{r=r_2}$, $\varepsilon_{\mathrm{t}}|_{r=r_3}$, and $\varepsilon_{\mathrm{t}}|_{r=r_4}$.

The first equation

From Eqs. a0′, b0, a1′, b1, a2′, b2, b3, c1, c2, and c3, we eliminate P_0, P_1, P_2, P_3, P_4, L_0, L_1, L_2, L_3, and L. Thus, we obtain the first equation

$$a_{11}\varepsilon_{\mathrm{L}} + a_{12}\varepsilon_{\mathrm{t}}\big|_{r=r_1} + a_{13}\varepsilon_{\mathrm{t}}\big|_{r=r_2} + a_{14}\varepsilon_{\mathrm{t}}\big|_{r=r_3} + a_{15}\varepsilon_{\mathrm{t}}\big|_{r=r_4} = b_{11}\varepsilon_1^{\mathrm{m}} + b_{12}\varepsilon_2^{\mathrm{m}} + b_{13}\varepsilon_3^{\mathrm{m}} + c_{11}\varepsilon_1^{\mathrm{f}} + c_{12}\varepsilon_2^{\mathrm{f}} + c_{13}\varepsilon_3^{\mathrm{f}} + d_{11}P_{\mathrm{L}} \tag{15}$$

where coefficients a_{11}, a_{12}, a_{13}, a_{14}, a_{15}, b_{11}, b_{12}, b_{13}, c_{11}, c_{12}, c_{13}, and d_{11} are respective functions whose concrete forms are composed of θ, ρ_1, ρ_2, ρ_3, $Q(=F/E_1)$, G_1, G_2, G_3, $M(=S_2/S_1)$, and $N(=S_3/S_2)$. Detailed shapes of those coefficients are described in the Appendix. P_{L} stands for the external force induced parallel to the wood fiber model, which is related to L_0, L_1, L_2, and L_3 as follows:

$$P_{\mathrm{L}} = 2\pi L = 2\pi\left(L_0 + L_1 + L_2 + L_3\right) = \int_{\substack{\text{crosscut}\\ \text{surface}}} \sigma_\ell r dr d\theta = 2\pi\int_{r_4}^{r_0} \sigma_\ell r dr$$

The second equation

ε_{L}, $\varepsilon_{\mathrm{t}}|_{r=r_1}$, $\varepsilon_{\mathrm{t}}|_{r=r_2}$, $\varepsilon_{\mathrm{t}}|_{r=r_3}$, and $\varepsilon_{\mathrm{t}}|_{r=r_4}$ are unknown variables to be solved as solutions of an algebraic equation (Eq. 15). To solve Eq. 15 for ε_{L}, $\varepsilon_{\mathrm{t}}|_{r=r_1}$, $\varepsilon_{\mathrm{t}}|_{r=r_2}$, $\varepsilon_{\mathrm{t}}|_{r=r_3}$, and $\varepsilon_{\mathrm{t}}|_{r=r_4}$, there must be at least four equations that are constituted by the same unknown variables. These equations can be derived from basic formula A.

From Eqs. a0′, a1′, a2′, a3, c1, and c2, we eliminate P_0, P_1, P_2, P_3, and P_4. Thus, we obtain

$$a_{21}\varepsilon_{\mathrm{L}} + a_{22}\varepsilon_{\mathrm{t}}\big|_{r=r_1} + a_{23}\varepsilon_{\mathrm{t}}\big|_{r=r_2} + a_{24}\varepsilon_{\mathrm{t}}\big|_{r=r_3} + a_{25}\varepsilon_{\mathrm{t}}\big|_{r=r_4} = b_{21}\varepsilon_1^{\mathrm{m}} + b_{22}\varepsilon_2^{\mathrm{m}} + b_{33}\varepsilon_3^{\mathrm{m}} + c_{21}\varepsilon_1^{\mathrm{f}} + c_{22}\varepsilon_2^{\mathrm{f}} + c_{23}\varepsilon_3^{\mathrm{f}} + d_{21}P_{\mathrm{L}} \tag{16}$$

The third equation

From Eqs. a0′, a1′, a2, a3, c1, and c2, we eliminate P_0, P_1, P_2, P_3, and P_4. Thus, we obtain

$$a_{31}\varepsilon_{\mathrm{L}} + a_{32}\varepsilon_{\mathrm{t}}\big|_{r=r_1} + a_{33}\varepsilon_{\mathrm{t}}\big|_{r=r_2} + a_{34}\varepsilon_{\mathrm{t}}\big|_{r=r_3} + a_{35}\varepsilon_{\mathrm{t}}\big|_{r=r_4} = b_{31}\varepsilon_1^{\mathrm{m}} + b_{32}\varepsilon_2^{\mathrm{m}} + b_{33}\varepsilon_3^{\mathrm{m}} + c_{31}\varepsilon_1^{\mathrm{f}} + c_{32}\varepsilon_2^{\mathrm{f}} + c_{33}\varepsilon_3^{\mathrm{f}} + d_{31}P_{\mathrm{L}} \tag{17}$$

The fourth equation

From Eqs. a0′, a1, a2, a3, c1, and c2, we eliminate P_0, P_1, P_2, P_3, and P_4. Thus, we obtain

$$a_{41}\varepsilon_{\mathrm{L}} + a_{42}\varepsilon_{\mathrm{t}}\big|_{r=r_1} + a_{43}\varepsilon_{\mathrm{t}}\big|_{r=r_2} + a_{44}\varepsilon_{\mathrm{t}}\big|_{r=r_3} + a_{45}\varepsilon_{\mathrm{t}}\big|_{r=r_4} = b_{41}\varepsilon_1^{\mathrm{m}} + b_{42}\varepsilon_2^{\mathrm{m}} + b_{43}\varepsilon_3^{\mathrm{m}} + c_{41}\varepsilon_1^{\mathrm{f}} + c_{42}\varepsilon_2^{\mathrm{f}} + c_{43}\varepsilon_3^{\mathrm{f}} + d_{41}P_{\mathrm{L}} \tag{18}$$

The fifth equation

From Eqs. a0′, a1′, a2′, a3′, c1, and c2, we eliminate P_0, P_1, P_2, P_3, and P_4. Thus, we obtain

$$a_{51}\varepsilon_{\mathrm{L}} + a_{52}\varepsilon_{\mathrm{t}}\big|_{r=r_1} + a_{53}\varepsilon_{\mathrm{t}}\big|_{r=r_2} + a_{54}\varepsilon_{\mathrm{t}}\big|_{r=r_3} + a_{55}\varepsilon_{\mathrm{t}}\big|_{r=r_4} = b_{51}\varepsilon_1^{\mathrm{m}} + b_{52}\varepsilon_2^{\mathrm{m}} + b_{53}\varepsilon_3^{\mathrm{m}} + c_{51}\varepsilon_1^{\mathrm{f}} + c_{52}\varepsilon_2^{\mathrm{f}} + c_{53}\varepsilon_3^{\mathrm{f}} + d_{51}P_{\mathrm{L}} \tag{19}$$

where coefficients a_{21}–a_{55}, b_{21}–b_{53}, c_{11}–c_{53}, and d_{11}–d_{51} are respective functions whose concrete forms are described in the Appendix.

Equations 15–19 constitute the simultaneous algebraic equations whose unknown variables are ε_{L}, $\varepsilon_{\mathrm{t}}^{r_1}(=\varepsilon_t|_{r=r_1})$, $\varepsilon_{\mathrm{t}}^{r_2}(=\varepsilon_t|_{r=r_2})$, $\varepsilon_{\mathrm{t}}^{r_3}(=\varepsilon_t|_{r=r_3})$, and $\varepsilon_{\mathrm{t}}^{r_4}(=\varepsilon_t|_{r=r_4})$. The values of $\varepsilon_1^{\mathrm{m}}$, $\varepsilon_2^{\mathrm{m}}$, $\varepsilon_3^{\mathrm{m}}$, $\varepsilon_1^{\mathrm{f}}$, $\varepsilon_2^{\mathrm{f}}$, $\varepsilon_3^{\mathrm{f}}$, and P_{L} should be given in advance. From the simultaneous equations, the solutions should be expressed in the following forms:

$$\begin{aligned}
\varepsilon_{\mathrm{L}} &= f_{11}(\mathbf{p})\varepsilon_1^{\mathrm{m}} + f_{12}(\mathbf{p})\varepsilon_2^{\mathrm{m}} + f_{13}(\mathbf{p})\varepsilon_3^{\mathrm{m}} + f_{14}(\mathbf{p})\varepsilon_1^{\mathrm{f}} + f_{15}(\mathbf{p})\varepsilon_2^{\mathrm{f}} + f_{16}(\mathbf{p})\varepsilon_3^{\mathrm{f}} + f_{17}(\mathbf{p})P_{\mathrm{L}} \\
\varepsilon_{\mathrm{t}}^{r_1} &= f_{21}(\mathbf{p})\varepsilon_1^{\mathrm{m}} + f_{22}(\mathbf{p})\varepsilon_2^{\mathrm{m}} + f_{23}(\mathbf{p})\varepsilon_3^{\mathrm{m}} + f_{24}(\mathbf{p})\varepsilon_1^{\mathrm{f}} + f_{25}(\mathbf{p})\varepsilon_2^{\mathrm{f}} + f_{26}(\mathbf{p})\varepsilon_3^{\mathrm{f}} + f_{27}(\mathbf{p})P_{\mathrm{L}} \\
\varepsilon_{\mathrm{t}}^{r_2} &= f_{31}(\mathbf{p})\varepsilon_1^{\mathrm{m}} + f_{32}(\mathbf{p})\varepsilon_2^{\mathrm{m}} + f_{33}(\mathbf{p})\varepsilon_3^{\mathrm{m}} + f_{34}(\mathbf{p})\varepsilon_1^{\mathrm{f}} + f_{35}(\mathbf{p})\varepsilon_2^{\mathrm{f}} + f_{36}(\mathbf{p})\varepsilon_3^{\mathrm{f}} + f_{37}(\mathbf{p})P_{\mathrm{L}} \\
\varepsilon_{\mathrm{t}}^{r_3} &= f_{41}(\mathbf{p})\varepsilon_1^{\mathrm{m}} + f_{42}(\mathbf{p})\varepsilon_2^{\mathrm{m}} + f_{43}(\mathbf{p})\varepsilon_3^{\mathrm{m}} + f_{44}(\mathbf{p})\varepsilon_1^{\mathrm{f}} + f_{45}(\mathbf{p})\varepsilon_2^{\mathrm{f}} + f_{46}(\mathbf{p})\varepsilon_3^{\mathrm{f}} + f_{47}(\mathbf{p})P_{\mathrm{L}} \\
\varepsilon_{\mathrm{t}}^{r_4} &= f_{51}(\mathbf{p})\varepsilon_1^{\mathrm{m}} + f_{52}(\mathbf{p})\varepsilon_2^{\mathrm{m}} + f_{53}(\mathbf{p})\varepsilon_3^{\mathrm{m}} + f_{54}(\mathbf{p})\varepsilon_1^{\mathrm{f}} + f_{55}(\mathbf{p})\varepsilon_2^{\mathrm{f}} + f_{56}(\mathbf{p})\varepsilon_3^{\mathrm{f}} + f_{57}(\mathbf{p})P_{\mathrm{L}}
\end{aligned} \tag{20}$$

where coefficients f_{11}–f_{57} are functions of $\mathbf{p}$, and $\mathbf{p}$ is a parameter vector whose components are θ, ρ_1, ρ_2, ρ_3, Q, G_1, G_2, G_3, M, and N. Among the solutions, ε_{L} represents the strain of the G-fiber model in the axial direction. According to the condition C4, the wood fiber model deforms axisymmetrically so that $\varepsilon_{\mathrm{t}}^{r_1}(=\varepsilon_{\mathrm{t}}^{r_0})$, $\varepsilon_{\mathrm{t}}^{r_2}$, $\varepsilon_{\mathrm{t}}^{r_3}$, and $\varepsilon_{\mathrm{t}}^{r_4}$ are equivalent strains to the diametral deformations at their respective radii. These strains are induced by a certain biomechanical change in the G-fiber. The thickness of the CML is small enough to be negligible if compared to those of the S1 and S2 layers. Therefore, $\varepsilon_{\mathrm{t}}^{r_1}$ can be regarded as the strain of the diameter in the wood fiber model ($=\varepsilon_{\mathrm{T}}$).

Developing Eqs. 20 into differential equations

According to assumption A2, Eqs. 20 are valid under the condition that the biomechanical change is infinitesimally small enough to be neglected. This means that ε_{L}, $\varepsilon_{\mathrm{t}}^{r_1}$, $\varepsilon_{\mathrm{t}}^{r_2}$, $\varepsilon_{\mathrm{t}}^{r_3}$, and $\varepsilon_{\mathrm{t}}^{r_4}$ in addition to $\varepsilon_1^{\mathrm{m}}$, $\varepsilon_2^{\mathrm{m}}$, $\varepsilon_3^{\mathrm{m}}$, $\varepsilon_1^{\mathrm{f}}$, $\varepsilon_2^{\mathrm{f}}$, $\varepsilon_3^{\mathrm{f}}$, and P_{L} in Eqs. 20 should be replaced as differential quantities, i.e., $d\varepsilon_{\mathrm{L}}$, $d\varepsilon_{\mathrm{t}}^{r_1}$, $d\varepsilon_{\mathrm{t}}^{r_2}$, $d\varepsilon_{\mathrm{t}}^{r_3}$, $d\varepsilon_{\mathrm{t}}^{r_4}$, $d\varepsilon_1^{\mathrm{m}}$, $d\varepsilon_2^{\mathrm{m}}$, $d\varepsilon_3^{\mathrm{m}}$, $d\varepsilon_1^{\mathrm{f}}$, $d\varepsilon_2^{\mathrm{f}}$, $d\varepsilon_3^{\mathrm{f}}$, and dP_{L}. Then, each expression in Eqs. 20 should be rewritten as a simple differential form, e.g.,

$$\begin{aligned}
d\varepsilon_{\mathrm{L}} &= f_{11}(\mathbf{p})d\varepsilon_1^{\mathrm{m}} + f_{12}(\mathbf{p})d\varepsilon_2^{\mathrm{m}} + f_{13}(\mathbf{p})d\varepsilon_3^{\mathrm{m}} + f_{14}(\mathbf{p})d\varepsilon_1^{\mathrm{f}} \\
&\quad + f_{15}(\mathbf{p})d\varepsilon_2^{\mathrm{f}} + f_{16}(\mathbf{p})d\varepsilon_3^{\mathrm{f}} + f_{17}(\mathbf{p})dP_{\mathrm{L}}
\end{aligned} \tag{20′}$$

The Eqs. 20′ are divided by dt, and are converted into the following differential equations:

$$\begin{aligned}
\dot{\varepsilon}_{\mathrm{L}} &= f_{11}(\mathbf{p})\dot{\varepsilon}_1^{\mathrm{m}} + f_{12}(\mathbf{p})\dot{\varepsilon}_2^{\mathrm{m}} + f_{13}(\mathbf{p})\dot{\varepsilon}_3^{\mathrm{m}} + f_{14}(\mathbf{p})\dot{\varepsilon}_1^{\mathrm{f}} + f_{15}(\mathbf{p})\dot{\varepsilon}_2^{\mathrm{f}} + f_{16}(\mathbf{p})\dot{\varepsilon}_3^{\mathrm{f}} + f_{17}(\mathbf{p})\dot{P}_{\mathrm{L}} \\
\dot{\varepsilon}_{\mathrm{t}}^{r_1} &= f_{21}(\mathbf{p})\dot{\varepsilon}_1^{\mathrm{m}} + f_{22}(\mathbf{p})\dot{\varepsilon}_2^{\mathrm{m}} + f_{23}(\mathbf{p})\dot{\varepsilon}_3^{\mathrm{m}} + f_{24}(\mathbf{p})\dot{\varepsilon}_1^{\mathrm{f}} + f_{25}(\mathbf{p})\dot{\varepsilon}_2^{\mathrm{f}} + f_{26}(\mathbf{p})\dot{\varepsilon}_3^{\mathrm{f}} + f_{27}(\mathbf{p})\dot{P}_{\mathrm{L}} \\
\dot{\varepsilon}_{\mathrm{t}}^{r_2} &= f_{31}(\mathbf{p})\dot{\varepsilon}_1^{\mathrm{m}} + f_{32}(\mathbf{p})\dot{\varepsilon}_2^{\mathrm{m}} + f_{33}(\mathbf{p})\dot{\varepsilon}_3^{\mathrm{m}} + f_{34}(\mathbf{p})\dot{\varepsilon}_1^{\mathrm{f}} + f_{35}(\mathbf{p})\dot{\varepsilon}_2^{\mathrm{f}} + f_{36}(\mathbf{p})\dot{\varepsilon}_3^{\mathrm{f}} + f_{37}(\mathbf{p})\dot{P}_{\mathrm{L}} \\
\dot{\varepsilon}_{\mathrm{t}}^{r_3} &= f_{41}(\mathbf{p})\dot{\varepsilon}_1^{\mathrm{m}} + f_{42}(\mathbf{p})\dot{\varepsilon}_2^{\mathrm{m}} + f_{43}(\mathbf{p})\dot{\varepsilon}_3^{\mathrm{m}} + f_{44}(\mathbf{p})\dot{\varepsilon}_1^{\mathrm{f}} + f_{45}(\mathbf{p})\dot{\varepsilon}_2^{\mathrm{f}} + f_{46}(\mathbf{p})\dot{\varepsilon}_3^{\mathrm{f}} + f_{47}(\mathbf{p})\dot{P}_{\mathrm{L}} \\
\dot{\varepsilon}_{\mathrm{t}}^{r_4} &= f_{51}(\mathbf{p})\dot{\varepsilon}_1^{\mathrm{m}} + f_{52}(\mathbf{p})\dot{\varepsilon}_2^{\mathrm{m}} + f_{53}(\mathbf{p})\dot{\varepsilon}_3^{\mathrm{m}} + f_{54}(\mathbf{p})\dot{\varepsilon}_1^{\mathrm{f}} + f_{55}(\mathbf{p})\dot{\varepsilon}_2^{\mathrm{f}} + f_{56}(\mathbf{p})\dot{\varepsilon}_3^{\mathrm{f}} + f_{57}(\mathbf{p})\dot{P}_{\mathrm{L}}
\end{aligned} \tag{21}$$

where the raised dot notation represents the derivative by t. Furthermore, ρ_1, ρ_2, and ρ_3 among the components of $\mathbf{p}$ should be rewritten into the differential quantities $\mathrm{d}\rho_1$, $\mathrm{d}\rho_2$, and $\mathrm{d}\rho_3$, because they depend on the elapsed time during a certain biomechanical change. Due to the assumption of axisymmetrical deformation, the following relations are inquired among respective layers:

$$\begin{aligned}
\rho_1 + d\rho_1 &= \frac{r_1 + dr_1}{r_2 + dr_2} = \frac{1 + d\varepsilon_{\mathrm{t}}^{r_1}}{1 + d\varepsilon_{\mathrm{t}}^{r_2}}\rho_1, \\
\rho_2 + d\rho_2 &= \frac{r_2 + dr_2}{r_3 + dr_3} = \frac{1 + d\varepsilon_{\mathrm{t}}^{r_2}}{1 + d\varepsilon_{\mathrm{t}}^{r_3}}\rho_2, \\
\rho_3 + d\rho_3 &= \frac{r_3 + dr_3}{r_4 + dr_4} = \frac{1 + d\varepsilon_{\mathrm{t}}^{r_3}}{1 + d\varepsilon_{\mathrm{t}}^{r_4}}\rho_3
\end{aligned} \tag{22}$$

Because $d\rho_3 d\varepsilon_{\mathrm{t}}^{r_4}$, $d\rho_2 d\varepsilon_{\mathrm{t}}^{r_3}$, and $d\rho_1 d\varepsilon_{\mathrm{t}}^{r_2}$ are regarded as higher order infinitesimal quantities, from Eqs. 22, we can obtain the following differential forms:

$$\begin{aligned}
d\rho_1 &= \left(d\varepsilon_{\mathrm{t}}^{r_1} - d\varepsilon_{\mathrm{t}}^{r_2}\right)\rho_1, \quad d\rho_2 = \left(d\varepsilon_{\mathrm{t}}^{r_2} - d\varepsilon_{\mathrm{t}}^{r_3}\right)\rho_2, \\
d\rho_3 &= \left(d\varepsilon_{\mathrm{t}}^{r_3} - d\varepsilon_{\mathrm{t}}^{r_4}\right)\rho_3
\end{aligned} \tag{22′}$$

These equations can be rewritten as differential equations of t as follows:

$$\dot{\rho}_1 = \left(\dot{\varepsilon}_{\mathrm{t}}^{r_1} - \dot{\varepsilon}_{\mathrm{t}}^{r_2}\right)\rho_1, \quad \dot{\rho}_2 = \left(\dot{\varepsilon}_{\mathrm{t}}^{r_2} - \dot{\varepsilon}_{\mathrm{t}}^{r_3}\right)\rho_2, \quad \dot{\rho}_3 = \left(\dot{\varepsilon}_{\mathrm{t}}^{r_3} - \dot{\varepsilon}_{\mathrm{t}}^{r_4}\right)\rho_3 \tag{23}$$

Equations 21 and 23 constitute a system of simultaneous differential equations whose unknown functions are ε_{L}, $\varepsilon_{\mathrm{t}}^{r_1}$, $\varepsilon_{\mathrm{t}}^{r_2}$, $\varepsilon_{\mathrm{t}}^{r_3}$, $\varepsilon_{\mathrm{t}}^{r_4}$, ρ_1, ρ_2, and ρ_3. On the other hand, $\varepsilon_1^{\mathrm{m}}$, $\varepsilon_2^{\mathrm{m}}$, $\varepsilon_3^{\mathrm{m}}$, $\varepsilon_1^{\mathrm{f}}$, $\varepsilon_2^{\mathrm{f}}$, $\varepsilon_3^{\mathrm{f}}$, and P_{L} are the functions whose t-dependent shapes should be given in advance.

Solving the simultaneous differential equations (Eqs. 21 and 23)

Solutions

Equations 21 and 23 give the deformation of the wood fiber model, which is induced by a certain biomechanical change occurring in the cell wall. In our case, examples of biomechanical change are the growth strains (maturation strains) during cell wall lignification, which is measured as the released strains of the growth stress; the swelling strains due to moisture adsorption; and the elastic deformation caused by external load.

We assume that change in the physical state in the cell wall starts at $t = 0$ and ends at $t = Z$. By integrating Eqs. 21 and 23 from $t = 0$ to $t = Z$, we can solve them for ε_L, ε_t^{r1}, ε_t^{r2}, ε_t^{r3}, ε_t^{r4}, ρ_1, ρ_2, and ρ_3. As the initial conditions at $t = 0$, we assume

$$\begin{aligned} &\varepsilon_L(0) = \varepsilon_t^{r1}(0) = \varepsilon_t^{r2}(0) = \varepsilon_t^{r3}(0) = \varepsilon_t^{r4}(0) = 0, \\ &\rho_1(0) = \hat{\rho}_1, \quad \rho_2(0) = \hat{\rho}_2, \quad \rho_3(0) = \hat{\rho}_3 \end{aligned} \tag{24}$$

Then, we divide the integral interval into n small parts, and denote the integrals of Eqs. 21 in the i-th small interval $[(i-1)Z/n < t < iZ/n,\ i = 1, 2, \ldots, n]$ as $\Delta^i\varepsilon_L$, $\Delta^i\varepsilon_t^{r1}$, $\Delta^i\varepsilon_t^{r2}$, $\Delta^i\varepsilon_t^{r3}$, and $\Delta^i\varepsilon_t^{r4}$. For example, $\Delta^i\varepsilon_L$ is calculated as

$$\begin{aligned} \Delta^i\varepsilon_L &\equiv \int_{(i-1)Z/n}^{i\cdot Z/n} \frac{d\varepsilon_L}{dt}dt \\ &= \int_{(i-1)Z/n}^{i\cdot Z/n} \Big(f_{11}(\mathbf{p})\dot{\varepsilon}_1^m + f_{12}(\mathbf{p})\dot{\varepsilon}_2^m + f_{13}(\mathbf{p})\dot{\varepsilon}_3^m + f_{14}(\mathbf{p})\dot{\varepsilon}_1^f \\ &\quad + f_{15}(\mathbf{p})\dot{\varepsilon}_2^f + f_{16}(\mathbf{p})\dot{\varepsilon}_3^f + f_{17}(\mathbf{p})\dot{P}_L\Big)dt \end{aligned} \tag{25}$$

In each small integral interval, the functions $\varepsilon_1^m(t)$, $\varepsilon_2^m(t)$, $\varepsilon_3^m(t)$, $\varepsilon_1^f(t)$, $\varepsilon_2^f(t)$, $\varepsilon_3^f(t)$, and respective components in $\mathbf{p}$, including ρ_1, ρ_2, and ρ_3, must be given in advance. However, ρ_1, ρ_2, and ρ_3 are unknown functions to be solved from simultaneous differential Eqs. 21 and 23. The values of ρ_1, ρ_2, and ρ_3, which should be used in the i-th small interval, can be estimated in the following process. At first, we integrate Eqs. 23 in the $(i-1)$-th small interval. Then, we obtain

$$\int_{(i-2)Z/n}^{(i-1)Z/n} \frac{d\rho_1}{dt}dt\Big(\equiv\Delta^{i-1}\rho_1\Big) = \left\{\int_{(i-2)Z/n}^{(i-1)Z/n}\left(\frac{d\varepsilon_t^{r1}}{dt} - \frac{d\varepsilon_t^{r2}}{dt}\right)\cdot\rho_1(t)dt\right\}$$

If n is taken as a large enough number, this equation gives

$$\Delta^{i-1}\rho_1 = \Big(\Delta^{i-1}\varepsilon_t^{r1} - \Delta^{i-1}\varepsilon_t^{r2}\Big)\cdot\rho_1^{i-2} \tag{26}$$

where ρ_1^{i-2} is equal to $\rho_1(t)$ at $t = (i-2)Z/n$. Thus, the value of ρ_1^{i-1}, which is $\rho_1(t)$ in the i-th small interval, is given as

$$\rho_1^{i-1} = \rho_1^{i-2} + \Delta^{i-1}\rho_1 = \Big(1 + \Delta^{i-1}\varepsilon_t^{r1} - \Delta^{i-1}\varepsilon_t^{r2}\Big)\cdot\rho_1^{i-2} \tag{27}$$

By using simultaneous recurrence equations (Eqs. 25 and 27), we can integrate simultaneous differential Eqs. 21 and 23 numerically.

Thus, the natural strain of the deforming wood fiber model at a certain time t $(= j\cdot Z/n,\ j$ is positive integer smaller than $n)$ can be derived as follows:

$$\begin{aligned} \varepsilon_L(t) &\equiv \lim_{n\to\infty}\sum_{i=1}^{j}\Delta^i\varepsilon_L = \int_0^t \frac{d\varepsilon_L}{dt}dt, \\ \varepsilon_T(t) &\equiv \lim_{n\to\infty}\sum_{i=1}^{j}\Delta^i\varepsilon_t^{r1} = \int_0^t \frac{d\varepsilon_t^{r1}}{dt}dt \end{aligned} \tag{28}$$

Strains $\varepsilon_L(t)$ and $\varepsilon_T(t)$ give natural strains of the dimensional changes induced in the wood fiber model. However, the released strain of the growth stress and the swelling due to water sorption are measured as the nominal strains in the deforming wood specimen. Then, we need to solve Eqs. 21 and 23 to give anisotropic dimensional changes of the wood fiber model as nominal strains.

The nominal strain of the deforming wood fiber model at a certain time t $(= j\cdot Z/n)$ in respective directions can be derived as follows:

$$\begin{aligned} \alpha(t) &= \lim_{n\to\infty}\left[\prod_{i=1}^{j}\Big(1 + \Delta^i\varepsilon_L\Big) - 1\right], \\ \beta(t) &= \lim_{n\to\infty}\left[\prod_{i=1}^{j}\Big(1 + \Delta^i\varepsilon_t^{r1}\Big) - 1\right] \end{aligned} \tag{29}$$

If the values of $\alpha(Z)$ and $\beta(Z)$ are smaller than 1%, changes of ρ_1, ρ_2, and ρ_3 are small enough to be neglected. In that case, we can obtain the $\alpha(t)$ and $\beta(t)$ from the first and the second formulae of Eqs. 21, which simplifies Eqs. 29 as follows:

$$\alpha(t) \cong \lim_{n\to\infty}\sum_{i=1}^{j}\Delta^i\varepsilon_L = \int_0^t\frac{d\varepsilon_L}{dt}dt, \quad \beta(t) \cong \lim_{n\to\infty}\sum_{i=1}^{j}\Delta^i\varepsilon_t^{r1} = \int_0^t\frac{d\varepsilon_t^{r1}}{dt}dt \tag{30}$$

Examples of simulations

Generation of the maturation strains due to cell wall lignification

Soon after the deposition of the CMF and the highly oriented polysaccharide framework in the secondary wall of the tracheid or libriform wood fiber, the matrix substance of hemicellulose and lignin deposits among the gaps of the framework bundle. In this process, the wood fiber tends to swell or shrink anisotropically, which generates anisotropic growth stress in the newly formed xylem. This is because free deformation of the individual fiber is restricted to inside the actual xylem. This process was formulated by using a wood fiber model of the CML, S1, S2, and G layers. In this case, irreversible deposition of the MT substance and the maturation of the CMF framework are postulated to cause a change in the biomechanical state of the tracheid or libriform fiber wall.

In the present study, the free dimensional change of the G-fiber is simulated during the wall maturation. P_L should be null in Eqs. 21. The integral interval is from the deposi-

Table 3. Assumed values for the chemical compositions in each layer of the green G-fiber wall

Layer	Cellulose crystal	Oriented polyose (non-crystalline) in the poly-saccharide framework	Isotropic matrix	Crystallinity in the polysaccharide framework
CML	15 (%)	0 (%)	85 (%)	100 (%)
S1	15	5	80	75
S2	30	10	60	75
G				
Case a	40	40	20	50
Case b	60	20	20	75
Case c	80	0	20	100

tions of the CMF framework ($t = 0$) to the completion of the G-fiber wall ($t = Z$). In this interval, the t-dependent patterns of ε_1^m, ε_2^m, ε_3^m, ε_1^f, ε_2^f, ε_3^f, and every component in **p** should be given in advance. As the initial conditions at $t = 0$, we adopt Eq. 24. According to the observations, the released strains of the growth stress are less than 0.5% both in the ℓ and the t directions. Then, the simplified formulae (Eqs. 30) can be used instead of Eqs. 29 when simulating the maturation strains $\alpha(t)|_{t=Z}$ and $\beta(t)|_{t=Z}$. In such a case, $\rho_1(t)$, $\rho_2(t)$, and $\rho_3(t)$ are regarded as approximately constant.

As the preliminary simulation, we calculated the values of $\alpha(t)|_{t=Z}$ ($\cong\varepsilon_L$) and $\beta(t)|_{t=Z}$ ($\cong\varepsilon_T$) under the conditions of the parameters assumed in Tables 3 and 4. The values in Tables 3 and 4, except those related to the G-layer, were used in our previous simulations on the generation of growth strains in the latewood tracheid of sugi (*Cryptomeria japonica*).[8] In the present simulation, the various cases for the percentage of the cellulose crystal in the G-layer are displayed in Table 3, and the relationship between ε_L, ε_T and $\varepsilon_3^f(t)|_{t=Z}$ was calculated for each case of framework crystallinity.

The result is shown in Fig. 3. According to the observation in the normal fiber of the softwood or the hardwood xylem, the released strain of the surface growth stress becomes −0.02% to −0.06% in the longitudinal direction, and 0.05%–0.1% in the tangential direction. In the TW xylem, on the other hand, the longitudinal released strain often becomes several times as large as in the NW xylem, and in some species forming considerably thick G-layers, such as *Robinia pseudoacacia*, it exceeds −0.5%.[2] The present simulation explains these phenomena well when the G-layer is assumed to shrink considerably in its axial direction during the G-fiber maturation.

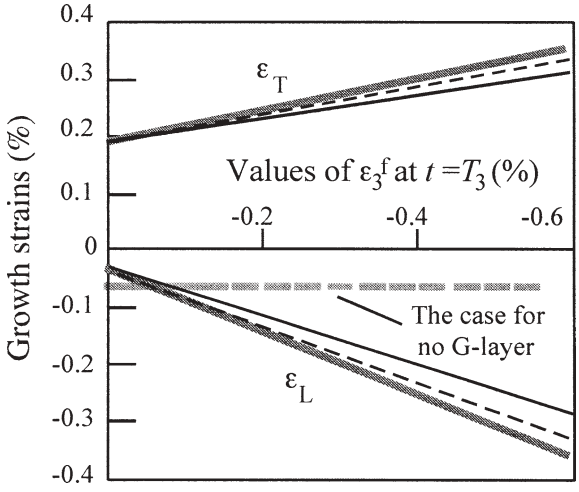

Fig. 3. An example of the simulation on the relations between the growth strains and the values of ε_3^f at $t = Z$ ($= T_3$) in the G-fiber. Values of the parameters assumed here are displayed in Table 4. Conditions for the crystallinity of the polysaccharide framework in the G-layer (see Table 3), *solid lines*, case a; *dashed lines*, case b; *shaded lines*, case c

Longitudinal elastic constants

At present, the longitudinal Young's modulus (E_L) of the wood fiber model is calculated based on Eqs. 21 and 23 under the assumption of the moisture steady state. Therefore, it is assumed that every component in **p** is constant. Moreover, $d\varepsilon_1^m$, $d\varepsilon_2^m$, $d\varepsilon_3^m$, $d\varepsilon_1^f$, $d\varepsilon_2^f$, and $d\varepsilon_3^f$ are all nil. Then, from Eqs. 21, we obtain the longitudinal Young's modulus of the G-fiber (E_L) as follows:

$$E_L = \frac{1}{\pi r_0^2}\frac{dP_L}{d\varepsilon_L} = \frac{1}{\pi r_0^2}\frac{1}{f_{17}(\mathbf{p})} \tag{31}$$

The substantial Young's modulus of the G-fiber can be calculated as

$$E_L^w = \frac{1}{\pi\left(r_0^2 - r_4^2\right)}\frac{dP_L}{d\varepsilon_L} = \frac{1}{\pi\left(r_0^2 - r_4^2\right)}\frac{1}{f_{17}(\mathbf{p})} \tag{31'}$$

In this case, an increase in the strain energy induced by external load is regarded as the biomechanical state change.

As a preliminary simulation, the values of E_L at $t = T_3$ were calculated under the conditions of the parameters given in Tables 3 and 4. The result is shown in Fig. 4. In the case in which the G-layer contains a certain amount of crystalline cellulose, calculated values of E_L become larger with the thickness of the G-layer; however, it is almost constant when the G-layer contains no crystalline cellulose.

Swelling and shrinkage strains due to the moisture adsorption

In the same way as the growth stress case, free dimensional change of the G-fiber due to moisture adsorption were simulated. Thus, P_L should be null in Eqs. 21. The integral interval is from the oven-dried state ($u = 0$) to the fiber

Table 4. Assumed values of the parameters for the simulation of the growth strains of the G-fiber

	E_0	E_1 (GPa)	E_2 (GPa)	E_3	S_0 (GPa)	S_1 (GPa)	S_2 (GPa)	S_3	ρ_0	ρ_1	ρ_2	ρ_3	ε_0^m	ε_1^m	ε_2^m	ε_3^m	ε_0^f	ε_1^f	ε_2^f	ε_3^f	θ (degrees)
$t = 0 \sim T_1$[a]	0	20.1	40.2	*[b]	3.92	Increase from 0 to 1.13	0	0	1.025	1.1	1.5	1.5	0	Increase to 1.0%	0	0	0	Increase from 0 to −0.15%	0	0	15
$t = T_1 \sim T_2$[a]	0	20.1	40.2	*	3.92	1.13	Increases to 0.933	0	1.025	1.1	1.5	1.5	0	–	Increase to 0.5%	0	0	–	Increase to −0.15%	0	15
$t = T_2 \sim T_3$[a]	0	20.1	40.2	*	3.92	1.13	0.933	Increases to a certain value[c]	1.025	1.1	1.5	1.5	0	–	–	0	0	–	–	Increases to a certain value	15

[a] The polysaccharide framework in the G-fiber is completed at $t = 0$. Deposition of the matrix substance in the S1 layer starts at $t = 0$, and ends at $t = T_1$. In the S2 layer, deposition of the matrix substance starts at $t = T_1$, and ends at $t = T_2$. Deposition of the matrix substance in the G-layer starts at $t = T_2$, and ends at $t = T_3$ ($= Z$), then the G-fiber is completed

[b] The value of E_3 is 53.6 GPa (from Case a in Table 3), 80.4 GPa (Case b), 107.2 GPa (Case c)

[c] The value of S_3 is 0.8 GPa (from Case a in Table 3), 0.533 GPa (Case b), 0.267 GPa (Case c)

Fig. 4. An example of the simulation on the relations between the longitudinal Young's modulus and the value of ρ_3 in the green G-fiber. Conditions for the crystallinity of the polysaccharide framework in the G-layer (see Table 3), *solid line*, case a; *dashed line*, case b; *shaded line*, case c

saturation point ($u = Z$). Therefore, it is regarded that the moisture content change u is equivalent to the elapsed time t. In the integral interval from $u = 0$ to $u = Z$, u-dependent patterns of ε_1^m, ε_2^m, ε_3^m, ε_1^f, ε_2^f, ε_3^f, and every component in **p** must be given in advance. In this case, the moisture sorption in the cell wall causes the biomechanical state change in the G-fiber.

The shrinkage strain of wood cannot be regarded as a reciprocal of the swelling strain because two different reference bases are used in their measurements. If the hysteresis effect between shrinkage and swelling processes is small enough to be neglected, we can convert the swellings $\alpha(u)$ and $\beta(u)$ into shrinkages $\alpha'(u)$ and $\beta'(u)$ at a certain moisture content (u) by using the following formulae:

$$\alpha'(u) = \frac{\alpha(Z) - \alpha(u)}{\alpha(Z) + 1}, \quad \beta'(u) = \frac{\beta(Z) - \beta(u)}{\beta(Z) + 1} \tag{32}$$

In the case that the oven-dried shrinkage of the wood becomes more than several percent in the transverse direction, we should use Eqs. 29 when calculating $\alpha(u)$ and $\beta(u)$ [or $\alpha'(u)$ and $\beta'(u)$].

In the same way as in the case of growth stress generation, we can reasonably expect that the longitudinal drying shrinkage $\alpha_L'(u)|_{u=Z}$ becomes considerably larger with the thickness of the G-layer and with the negative value of $\varepsilon_3^f|_{u=Z}$.

Concluding remarks

In the subsequent report, further concrete simulations will be demonstrated, and the results will be compared with the experimental results obtained from the TW of a 70-year-old Kohauchiwakaede (*Acer sieboldianum* Miq.), which are already reported.[3] Examples include high tensile growth stress generation, large longitudinal Young's modulus, and large axial shrinkage due to water desorption in the G-fiber.

Appendix

Detailed expressions of coefficients a_{11}–a_{55}; b_{11}–b_{53}; c_{11}–c_{53}; d_{11}–d_{51} in Eqs. 15–19.

$$a_{11} = \Omega_2\alpha + A + B + C,\quad a_{12} = D,\quad a_{13} = E,\quad a_{14} = -\frac{1}{6}\frac{\alpha}{\rho_2^2}\Lambda_2\left(\Lambda_2 - 2\Gamma_2\right),\quad a_{15} = 0,$$

$$b_{11} = H - \frac{\alpha X_1}{6M}\left(\Lambda_2 - 2\Gamma_2\right)\left(\frac{1}{\rho_2^2 - 1}\right)\left(\frac{\rho_1^2 - 1}{\rho_1^2}\right),\quad b_{12} = \alpha\cdot\Phi_2 - \frac{1}{6}\frac{X_2}{\rho_2^2}\alpha\left(\Lambda_2 - 2\Gamma_2\right),\quad b_{13} = \frac{1}{2}N\alpha\Lambda_2\left(\frac{1}{\rho_2^2 - 1}\right)\left(\frac{\rho_3^2 - 1}{\rho_3^2}\right),$$

$$c_{11} = I - \frac{\alpha\Delta_1}{6M}\left(\Lambda_2 - 2\Gamma_2\right)\left(\frac{1}{\rho_2^2 - 1}\right)\left(\frac{\rho_1^2 - 1}{\rho_1^2}\right),\quad c_{12} = \alpha\cdot\Sigma_2 - \frac{1}{6}\frac{\Delta_2}{\rho_2^2}\alpha\left(\Lambda_2 - 2\Gamma_2\right),,\quad c_{13} = \frac{1}{3}N\alpha\Lambda_2\left(\frac{1}{\rho_2^2 - 1}\right)\left(\frac{\rho_3^2 - 1}{\rho_3^2}\right)G_3,$$

$$d_{11} = \frac{2}{3}\frac{\Lambda_2}{M}\alpha\left(\frac{\rho_2^2}{\rho_2^2 - 1}\right)\frac{1}{S_1 r_2^2}\frac{1}{2\pi},\quad a_{21} = G_1Q + \frac{1}{2}\left(\frac{\rho_1^2 - 1}{\rho_1^2}\right)\Gamma_1 + \frac{M}{2}\left(\frac{\rho_2^2 - 1}{\rho_2^2}\right)\Gamma_2 + \frac{1}{2}MN\left(\rho_3^2 - 1\right),\quad a_{22} = 2G_1Q,$$

$$a_{23} = \frac{1}{2}\left(\frac{\rho_1^2 - 1}{\rho_1^2}\right)\Lambda_1,\quad a_{24} = \frac{M}{2}\left(\frac{\rho_2^2 - 1}{\rho_2^2}\right)\Lambda_2 + MN\left(\rho_3^2 - 1\right),\quad a_{25} = 0,\quad b_{21} = \frac{1}{2}\left(\frac{\rho_1^2 - 1}{\rho_1^2}\right)X_1,\quad b_{22} = \frac{M}{2}\left(\frac{\rho_2^2 - 1}{\rho_2^2}\right)X_2,$$

$$b_{23} = \frac{3}{2}MN\left(\rho_3^2 - 1\right),\quad c_{21} = \frac{1}{2}\left(\frac{\rho_1^2 - 1}{\rho_1^2}\right)\Delta_1,\quad c_{22} = \frac{M}{2}\left(\frac{\rho_2^2 - 1}{\rho_2^2}\right)\Delta_2,\quad c_{23} = 0,\quad d_{21} = 0,$$

$$a_{31} = G_1Q + \frac{1}{2}\left(\frac{\rho_1^2 - 1}{\rho_1^2}\right)\Gamma_1 + \frac{M}{2}\left(\rho_2^2 - 1\right)\Gamma_2' + \frac{1}{2}MN\left(\rho_3^2 - 1\right),\quad a_{32} = 2G_1Q,$$

$$a_{33} = \frac{1}{2}\left(\frac{\rho_1^2 - 1}{\rho_1^2}\right)\Lambda_1 + \frac{M}{2}\left(\rho_2^2 - 1\right)\Lambda_2,\quad a_{34} = MN\left(\rho_3^2 - 1\right),\quad a_{35} = 0,\quad b_{31} = \frac{1}{2}\left(\frac{\rho_1^2 - 1}{\rho_1^2}\right)X_1,\quad b_{32} = \frac{M}{2}\left(\rho_2^2 - 1\right)X_2',$$

$$b_{33} = \frac{3}{2}MN\left(\rho_3^2 - 1\right),\quad c_{31} = \frac{1}{2}\left(\frac{\rho_1^2 - 1}{\rho_1^2}\right)\Delta_1,\quad c_{32} = \frac{M}{2}\left(\rho_2^2 - 1\right)\Delta_2',\quad c_{33} = 0,\quad d_{31} = 0,$$

$$a_{41} = G_1Q + \frac{1}{2}\left(\rho_1^2 - 1\right)\Gamma_1' + \frac{M}{2}\left(\rho_2^2 - 1\right)\Gamma_2' + \frac{1}{2}MN\left(\rho_3^2 - 1\right),\quad a_{42} = 2G_1Q + \frac{1}{2}\left(\rho_1^2 - 1\right)\Lambda_1,\quad a_{43} = \frac{M}{2}\left(\rho_2^2 - 1\right)\Lambda_2,$$

$$a_{44} = MN\left(\rho_3^2 - 1\right),\quad a_{45} = 0,\quad b_{41} = \frac{1}{2}\left(\rho_1^2 - 1\right)X_1',\quad b_{42} = \frac{M}{2}\left(\rho_2^2 - 1\right)X_2',\quad b_{43} = \frac{3}{2}MN\left(\rho_3^2 - 1\right),\quad c_{41} = \frac{1}{2}\left(\rho_1^2 - 1\right)\Delta_1',$$

$$c_{42} = \frac{M}{2}\left(\rho_2^2 - 1\right)\Delta_2',\quad c_{43} = 0,\quad d_{41} = 0,\quad a_{51} = G_1Q + \frac{1}{2}\left(\frac{\rho_1^2 - 1}{\rho_1^2}\right)\Gamma_1 + \frac{M}{2}\left(\frac{\rho_2^2 - 1}{\rho_2^2}\right)\Gamma_2 + \frac{1}{2}MN\left(\frac{\rho_3^2 - 1}{\rho_3^2}\right),$$

$$a_{52} = 2G_1Q,\quad a_{53} = \frac{1}{2}\left(\frac{\rho_1^2 - 1}{\rho_1^2}\right)\Lambda_1,\quad a_{54} = \frac{M}{2}\left(\frac{\rho_2^2 - 1}{\rho_2^2}\right)\Lambda_2,\quad a_{55} = MN\left(\frac{\rho_3^2 - 1}{\rho_3^2}\right),\quad b_{51} = \frac{1}{2}\left(\frac{\rho_1^2 - 1}{\rho_1^2}\right)X_1,$$

$$b_{52} = \frac{M}{2}\left(\frac{\rho_2^2 - 1}{\rho_2^2}\right)X_2,\quad b_{53} = \frac{3}{2}MN\left(\frac{\rho_3^2 - 1}{\rho_3^2}\right),\quad c_{51} = \frac{1}{2}\left(\frac{\rho_1^2 - 1}{\rho_1^2}\right)\Delta_1,\quad c_{52} = \frac{M}{2}\left(\frac{\rho_2^2 - 1}{\rho_2^2}\right)\Delta_2,\quad c_{53} = 0,\quad d_{51} = 0$$

Provided that detailed shapes of functions A, B, C, D, E, H, I, α, and β are as follows:

$$A = \frac{1}{M}\left(\frac{\Gamma_2'}{\Gamma_1}\right)\left(\frac{\rho_2^2}{\rho_2^2 - 1}\right)\left\{\left(\rho_1^2 - 1\right)\Omega_1 + \frac{2}{3}\rho_1^2 G_1 Q\left(-\Gamma_1' + 2\Lambda_1\right)\right\}$$

$$B = \frac{1}{M}\left(\frac{\Gamma_2'}{3}\right)\left(\frac{\rho_2^2}{\rho_2^2 - 1}\right)\beta\left(2G_1Q + \frac{\rho_1^2 - 1}{\rho_1^2}\Gamma_1\right),\quad \alpha = \left(\frac{\Gamma_2'}{\Gamma_1}\right)\left(\frac{\Lambda_1}{\Lambda_2}\right),\quad \beta = 1 - \alpha = 1 - \left(\frac{\Gamma_2'}{\Gamma_1}\right)\left(\frac{\Lambda_1}{\Lambda_2}\right),$$

$$C = -\alpha\left(\Lambda_2 - 2\Gamma_2\right)\left[\frac{1}{6}\frac{\Gamma_2}{\rho_2^2} + \frac{1}{6}\left(\frac{\Gamma_1}{M}\right)\left(\frac{1}{\rho_2^2 - 1}\right)\left(\frac{\rho_1^2 - 1}{\rho_1^2}\right) + \frac{1}{3}\left(\frac{1}{M}\right)\left(\frac{1}{\rho_2^2 - 1}\right)G_1Q\right]$$
$$+ \frac{1}{2}N\cdot\Lambda_2\cdot\alpha\left(\frac{1}{\rho_2^2 - 1}\right)\left(\frac{\rho_3^2 - 1}{\rho_3^2}\right)\left(1 + \frac{2}{3}G_3\right),$$

$$D = \frac{2}{3}\left(\frac{1}{\rho_2^2 - 1}\right)\left(\frac{1}{M}\right)\left[\rho_2^2\Gamma_2'\left(2\beta + \frac{\Lambda_1 - 2\Gamma_1'}{\Gamma_1}\rho_1^2\right) + \alpha\left(2\Gamma_2 - \Lambda_2\right)\right]G_1Q,$$

$$E = \frac{1}{6}\left(\frac{\Lambda_1}{M}\right)\left(\frac{1}{\rho_2^2 - 1}\right)\left(\frac{\rho_1^2 - 1}{\rho_1^2}\right)\left(2\Gamma_2'\beta\rho_2^2 - \alpha\left(\Lambda_2 - 2\Gamma_2\right)\right),$$

$$H = \left(\frac{\Gamma_2'}{M}\right)\left(\frac{\rho_2^2}{\rho_2^2 - 1}\right)\left(\frac{\rho_1^2 - 1}{\rho_1^2}\right)\left(\frac{\Phi_1}{\Gamma_1}\rho_1^2 + \frac{1}{3}\beta\cdot X_1\right),$$

$$I = \left(\frac{\Gamma_2'}{M}\right)\left(\frac{\rho_2^2}{\rho_2^2 - 1}\right)\left(\frac{\rho_1^2 - 1}{\rho_1^2}\right)\left(\frac{\Sigma_1}{\Gamma_1}\rho_1^2 + \frac{1}{3}\beta\cdot\Delta_1\right)$$

References

1. Okuyama T, Yamamoto H, Iguchi M, Yoshida M (1990) Generation process of growth stresses in cell walls. II. Growth stress in tension wood. Mokuzai Gakkaishi 36:797–803
2. Okuyama T, Yamamoto H, Yoshida M, Hattori Y, Archer RR (1994) Growth stresses in tension wood. Role of microfibrils and lignification. Ann For Sci 51:291–300
3. Yamamoto H, Okuyama T, Sugiyama K, Yoshida M (1992) Generation process of growth stresses in cell walls. IV. Action of the cellulose microfibrils upon the generation of the tensile stresses. Mokuzai Gakkaishi 38:107–113
4. Kollmann FFP, Cote Jr WA (1984) Principles of wood science and technology, vol I: solid wood. Springer, Berlin Heidelberg New York
5. Boyd JD (1977) Relationship between fiber morphology and shrinkage of wood. Wood Sci Technol 11:3–22
6. Norberg H, Meyer H (1966) Physical and chemical properties of the gelatinous layer in tension wood fibres of aspen (*Populus tremula* L.). Holzforschung 6:174–178
7. Scurfield G (1973) Reaction wood. Its structure and function. Science 179:647–655
8. Yamamoto H, Kojima Y, Okuyama T, Abasolo WP, Gril J (2002) Origin of the biomechanical properties of wood related to the fine structure of the multi-layered cell wall. J Biomech Eng Trans ASME 124:432–440
9. Yamamoto H, Kojima Y (2002) Properties of cell wall constituents in relation to longitudinal elasticity of wood. Part 1. Formulation of the longitudinal elasticity of an isolated wood fiber. Wood Sci Technol 36:55–74
10. Yamamoto H, Okuyama T, Yoshida M (1995) Generation process of growth stresses in cell walls. VI. Analysis of the growth stress generation by using cell model having three layers (S1, S2, and I + P). Mokuzai Gakkaishi 41:1–8
11. Yamamoto H (1998) Generation mechanism of growth stresses in wood cell walls: roles of lignin deposition and cellulose microfibril during cell wall maturation. Wood Sci Technol 32:171–182
12. Yamamoto H (1999) A model of the anisotropic swelling and shrinking process of wood. Part 1. Generalization of Barber's wood fiber model. Wood Sci Technol 33:311–325
13. Yamamoto H, Sassus F, Ninomiya M, Gril J (2001) A model of the anisotropic swelling and shrinking process of wood. Part 2. A simulation of shrinking wood. Wood Sci Technol 35:167–181
14. Kojima Y, Yamamoto H (2003) Properties of the cell wall constituents in relation to the longitudinal elasticity of wood. Part 2. Origin of the moisture dependency of the longitudinal elasticity of wood. Wood Sci Technol (in press)
15. Yamamoto H, Okuyama T, Yoshida M (1993) Generation process of growth stresses in cell walls. V. Model of tensile stress generation in gelatinous fibers. Mokuzai Gakkaishi 39:118–125
16. Liang CY, Bassett KH, McGiness EA, Marchessault RH (1960) Infrared spectra of crystalline polysaccharides. VII. Thin wood sections. TAPPI 43:1017–1024
17. Fushitani M (1973) Study of molecular orientation in wood by fluorescence method (in Japanese). Mokuzai Gakkaishi 19:135–140
18. Salmen L (2000) Structure – property relations for wood; from the cell wall polymeric arrangement to the macroscopic behavior. Proceedings of the third plant biomechanics conference, Freiburg-Badenweiler, pp 452–462
19. Barber NF, Meylan BA (1964) The anisotropic shrinkage of wood. A theoretical model. Holzforschung 18:146–156
20. Gril J, Sassus F, Yamamoto H, Guitard D (1999) Maturation and drying strain of wood in longitudinal direction: a single-fiber mechanical model. Proceedings of the third workshop "Connection between silviculture and wood quality through modelling approaches and simulation software". La Londe-Les-Maures, 309–314